

## A novel method for the fabrication of freestanding PZT features on substrates

Joost G. van Bennekom<sup>a</sup>, Louis Winnubst<sup>a</sup>, Wietze Nijdam<sup>b</sup>,  
Matthias Wessling<sup>a</sup>, Rob G.H. Lammertink<sup>a,\*</sup>

<sup>a</sup> Membrane Technology Group, Mesa+ institute for nanotechnology, University of Twente, P.O. Box 217, 7500 AE Enschede, The Netherlands

<sup>b</sup> Aquamarijn Microfiltration BV, Berkelkade 11, 7201 JE Zutphen, The Netherlands

Received 27 March 2009; received in revised form 27 May 2009; accepted 11 June 2009

Available online 14 July 2009

### Abstract

A simple and cheap micromoulding fabrication route was developed to prepare freestanding piezo active features. Dimensions as small as 200  $\mu\text{m}$  by 200  $\mu\text{m}$  and 40  $\mu\text{m}$  high were successfully fabricated via a replication technique. The lead zirconate titanate features were thoroughly characterized using SEM, EDX and XRD analysis. The properties of the features were influenced by several factors like the type of substrate, sintering temperature and sintering atmosphere. Features prepared on alumina substrates and sintered in lead atmosphere displayed a structure with reproducible dimensions. Next to that they were low in porosity and had a comparable composition with respect to the starting powder. The remanent polarization of the lead zirconate film was 12.3  $\mu\text{C}/\text{cm}^2$  and the coercive field was 8.7 kV/cm.

© 2009 Elsevier Ltd. All rights reserved.

**Keywords:** PZT; Micromoulding; Tape casting; Sintering; Substrates

### 1. Introduction

Lead zirconate titanate ( $\text{PbZr}_x\text{Ti}_{1-x}\text{O}_3$ ,  $0 \leq x \leq 1$ , PZT) is a ceramic material with excellent piezoelectric properties. There are several methods to pattern PZT thick films ( $>5 \mu\text{m}$ ) and to produce complex piezo ceramic structures.

Slip pressing and centrifugal casting are used to fabricate PZT arrays with high aspect ratio and dimensions in the 100  $\mu\text{m}$  range.<sup>1</sup> Another commonly used technique is direct green tape micromoulding.<sup>2,3–6</sup> In this case a PZT suspension is cast on a structured mould and adapts the inverse structure of the mould. After release from the mould and firing a structured PZT film is left. The casting methods described in the latter paragraph allow a wide variety of structures to be fabricated, however the PZT structures are always interconnected. Obtaining freestanding features requires secondary processing steps.

Freestanding green features can be fabricated by means of a sacrificial photoresist mould on top of a substrate.<sup>6</sup> The photoresist is locally exposed and developed to obtain the inverse

of the required structure. Subsequently, the mould is filled with suspension. The photoresist is either dissolved leaving the green compact in the required structure or burnt out followed by a sintering step. Lines with a height of 5  $\mu\text{m}$  and a width of 10  $\mu\text{m}$  can be prepared in this way, but each new experiment requires the preparation of a new photoresist mould.<sup>7</sup>

Screen printing does not make use of sacrificial moulds.<sup>2,8</sup> A suspension is printed through a screen on a substrate. The printed ink should meet certain requirements (e.g. viscosity, solvent evaporation rate). Structuring is somewhat limited by the ratio of dense and open areas of the screen and the dimensions of the printed features.<sup>9</sup> Limitations are even more severe when using ink jet printing of PZT.<sup>10,11</sup> Small orifices can clog and multiple printing steps are required with the additional drying issues for thicker structures.

More advanced techniques as pulsed laser deposition<sup>12</sup> (PLD) and aerosol deposition<sup>13</sup> allow the fabrication of freestanding features with shadow masking. An additional advantage is that PZT features can be grown *in situ* and epitaxially, which reduces the process temperature to 600 °C. The poling process, required for PZT produced from sol–gel or suspension casting, becomes superfluous.<sup>14</sup> Disadvantages of these techniques are the requirement of advanced equipment and

\* Corresponding author. Tel.: +31 53 4892063; fax: +31 53 4894611.  
E-mail address: [r.g.h.lammertink@tnw.utwente.nl](mailto:r.g.h.lammertink@tnw.utwente.nl) (R.G.H. Lammertink).

up-scaling difficulties. Typical film thicknesses of these deposition techniques are  $<0.5 \mu\text{m}$ , which is significantly smaller than the films fabricated with the other techniques mentioned.

This paper deals with a novel method in microstructuring PZT into freestanding features using a micromoulding technique. A suspension containing commercial PZT powder is moulded to the required features and released from the mould by casting an additional polymeric film over it. The resulting composite (polymeric film + moulded suspension) is subsequently fired leaving freestanding PZT features. The micromoulding technique allows a wide variety of shapes with dimensions in the lower micrometer range to be fabricated. Other advantages of this method include its simplicity, cost effectiveness and its up-scaling opportunities.

## 2. Experimental

### 2.1. Suspension preparation

A suspension suitable for tape casting was prepared according to the recipe given in Table 1. Commercial  $\text{Pb}(\text{Zr}_{0.53}\text{Ti}_{0.47})\text{O}_3$  powder supplied by Sparkler Ceramics, India and a dispersant, Solsperse 20000, were added to the solvent iso-propanol. The solution was ball milled for 24 h using zirconia balls (diameter 5 mm), to deagglomerate the powder. After addition of binder (polyvinyl butyral, PVB) and plasticizer (benzyl butyl phthalate, BBP) the suspension was mixed by means of the zirconia balls for 24 h. To remove bubbles from the suspension, the suspension was left standing for another 24 h. After this ‘degassing’ step, the suspension was constantly magnetically stirred in between different casting experiments to prevent sedimentation.

### 2.2. Fabrication of the green features

A schematic summary of the production process is displayed in Fig. 1. The suspension was cast on the mould (A) about twice the thickness of the depth of the features (B) and left for solvent evaporation. The excess on the ridges was removed by means of a double-edged razorblade (C). In a second casting step a polymer solution (PVB in iso-propanol) was cast and formed a composite green tape (D). The composite green tape was immersed in water and subsequently the tape was released from the mould by peeling and dried between glass plates for straightening (E). The tape was applied to a substrate (either a diced silicon wafer or a diced polished pure alumina wafer) which was wetted with ethanol. The substrate was heated to

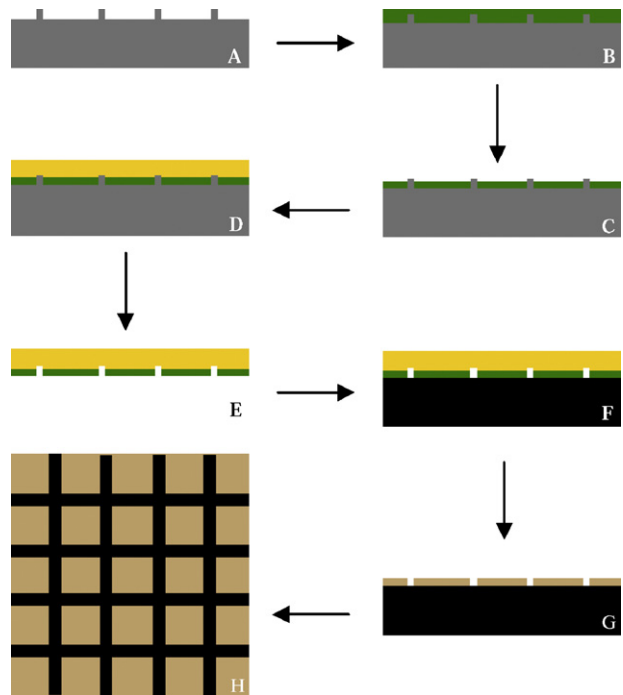


Fig. 1. Schematic cross-sectional overview of the preparation procedure: silicon mould (A), suspension cast on mould (B), solvent evaporation and shrinkage of the suspension (C), polymer film cast (D), release of the composite green tape (E), applying composite green tape on substrate (F), fired freestanding ceramic structures (G), top view freestanding features on substrate (H).

$100^\circ\text{C}$  for 5 min to melt the composite green tape to the substrate (F). Binder burn out and sintering were performed (G and H) after this heating treatment.

### 2.3. Binder burn out and sintering

Thermal gravimetric analysis (TGA, Setaram, Setsys 16) was carried out to determine the binder burn out procedure for the sintering process. An alumina cup was filled with a sample to perform the TGA measurement with. The heating ramp was  $10^\circ\text{C}/\text{min}$  till  $300^\circ\text{C}$  and  $0.5^\circ\text{C}/\text{min}$  from  $300^\circ\text{C}$  to  $550^\circ\text{C}$ . Weight-loss (binder burn out) started around  $250^\circ\text{C}$ . The TGA curve dropped sharply between  $300^\circ\text{C}$  and  $320^\circ\text{C}$ , then binder burn out speed diminished till the curves flattens out from  $430^\circ\text{C}$ .

In the sintering procedure of the composite tapes the heating rate was kept low ( $1^\circ\text{C}/\text{min}$ ) till  $500^\circ\text{C}$ . Binder burn out took place slowly to prevent distortion of the features by formation of gas bubbles. After a dwell of 30 min at  $500^\circ\text{C}$ , the heating rate was increased to  $4^\circ\text{C}/\text{min}$  till the final sinter temperature was reached ( $1000\text{--}1200^\circ\text{C}$  for 1–3 h). The cooling rate was  $5^\circ\text{C}/\text{min}$ . Sintering was performed in air or in lead atmosphere created by sintering the samples in the presence of  $\text{PbZrO}_3$  (PZ) powder in closed alumina crucibles.<sup>15</sup>

Other PZT samples were isostatically pressed at 4000 bar using a home-made pressure vessel with hydraulics (EPSI, Temse, Belgium) to determine the bulk material properties. The green samples were sintered at  $1200^\circ\text{C}$  for 3 h at a heating rate of

Table 1  
Recipe for slurry preparation<sup>3</sup> (wt%).

Function	Component	Comp.
Solvent	Iso-propanol (Merck, Germany)	32
Dispersant	Solsperse 20000 (Solsperse, England)	0.5
Powder	$\text{Pb}(\text{Zr}_{0.53}\text{Ti}_{0.47})\text{O}_3$ (Sparkler Ceramics, India)	61
Binder	Polyvinyl butyral (TCW, USA)	4.5
Plasticizer	Benzyl butyl phthalate (TCW, USA)	2.0

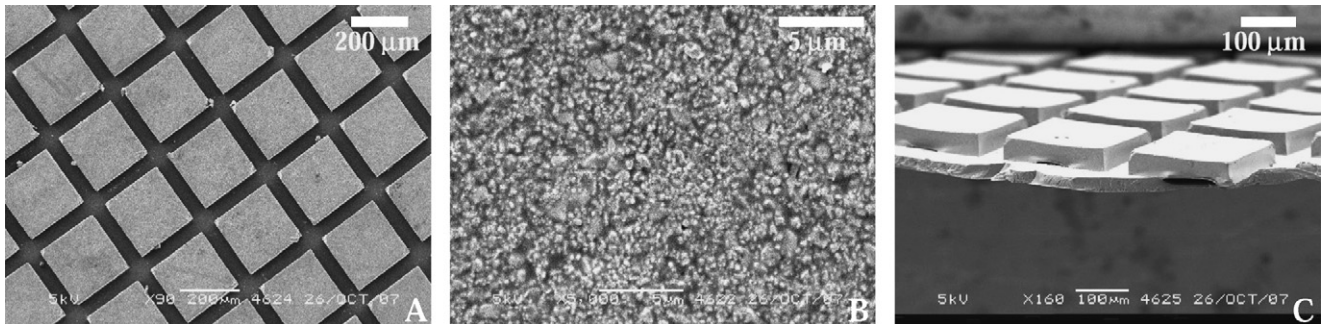


Fig. 2. SEM micrographs of a composite green tape. Top view (A), surface (B), cross-section (C).

4 °C/min followed by cooling at a rate of 5 °C/min. After sintering, discs were cut from the PZT sample, using a diamond saw. The thickness of the discs varies between 200 μm and 1300 μm and the diameter was approximately 16 mm.

#### 2.4. Characterization

The morphology of the sample was investigated by scanning electron microscopy (SEM) using a JEOL, JSM 5600 or a ZEISS, FE Leo 1550 microscope. The composition of the top 0.5–1.0 μm of the surface and the cross-section of a sample was determined by EDX (Thermo Noran Vantage 6). The EDX analysis of the sample surface was carried out at a magnification of 5000 on areas measuring 72 μm by 54 μm. For the composition determination of the cross-section a window of 20 μm by 2 μm was used. The composition was measured at three different parts in the cross-section: near the surface, in the middle of the sample and near the substrate. The crystal structure of both the starting powder and the sintered features was determined by XRD (Philips XRD X-pert). The material density of sintered PZT was determined using a Pycnometer (Micromeritics, AccuPyc 1330).

The porosity of a cross-section was determined by image analysis of a SEM micrograph.

#### 2.5. Electrical measurements

For electrical measurements a larger PZT film (3 mm by 5 mm and a thickness of 400 μm) was sintered on alumina and removed after sintering. The preparation procedure was otherwise equal

to the tape-casting method. To perform electrical measurements a gold electrode was sputtered using a Balzer sputter device (Union SCD 040) on both bottom and top of the PZT sample. Platinum wires (diameter 0.05 mm) were connected to the gold electrodes with silver paste (silver methyl-iso-butylketon, Acheson Electrodag). The PE hysteresis loops were measured using a Precision Pro Ferroelectric Analyzer (Radiant Technologies Inc.) with a high voltage amplifier. The analyzer was connected via clamps to the platinum wires. Measurements were performed in silicone oil (Aldrich, Germany) at room temperature.

### 3. Results and discussion

#### 3.1. The green state

Fig. 2 shows SEM micrographs of the composite green tape comprising the polymeric lift off film and the features containing PZT powder and polymer. The dimensions of the features are 200 μm by 200 μm (same dimensions as the structures on the mould). The thickness is approximately 40 μm. The features contain binder (7.4%), plasticizer (2.9%) and PZT powder (89.7%). The lift off film below the squares (Fig. 2A and C) is purely polymeric. The squares are sharply edged and powder density is high as shown in Fig. 2B. The powder particles are clearly visible on this SEM picture.

#### 3.2. Sintering on silicon substrates

SEM micrographs of features sintered on silicon for 1 h at 1000 °C can be seen in Fig. 3. The features lose their sharply

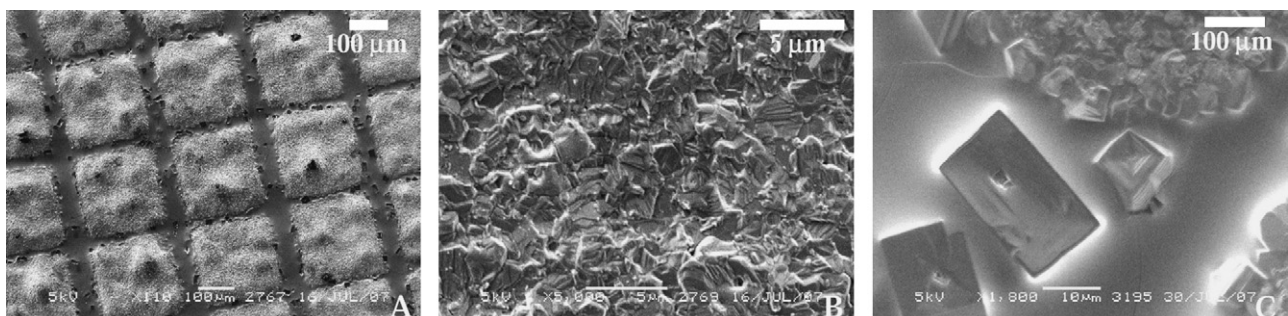


Fig. 3. SEM micrographs of sintered features on silicon sintered for 1 h at 1000 °C. Top view (A), surface (B), magnification of the crystals at the edges of the features (C).



Table 2  
Composition of features sintered on silicon in air atmosphere for 1 h at 1000 °C.

Comp.	Powder (suppl.)	Powder (EDX)	Feature
Pb	0.50	0.50	0.49
Zr	0.27	0.26	0.04
Ti	0.23	0.24	0.41
Si	–	–	0.06

The composition of the powder according to the supplier, determined by EDX (no temperature treatment carried out) and the composition of the sintered features.

edged shape and the surface contains several irregularities and large rectangular crystals. In the SEM analysis no pores were observed and it is hard to distinguish clear grains at the surface. EDX analysis showed that most of the rectangular crystals contain silicon, zirconium and oxygen. Some of them contain lead, silicon and oxygen.

Table 2 shows the composition of the powder according to the supplier and according to our EDX measurements. The composition determined by EDX, from the center of a feature is given. The presence of silicon in the features is ascribed to diffusion of silicon from the silicon substrate to the surface of the feature. EDX analysis of the cross-section showed a strong gradient in silicon from the substrate side of the sample to the surface of the sample.

At elevated temperatures silicon is not suited to be used as substrate for sintering PZT, because it is too reactive, confirming the results found by Beepy et al.<sup>16</sup> However, they did not report the formation of the rectangular crystals and silicon diffusion into the PZT.

### 3.3. Sintering on alumina substrates in air

Alumina is more stable than silicon in combination with lead zirconate titanate and can withstand higher temperatures than silicon.<sup>17,18</sup> PZT features were sintered in air at 1000 °C, 1100 °C and 1200 °C. Even after sintering at 1200 °C the features show high porosity (Fig. 4). Between the squares (Fig. 4A) there is some PZT material visible which is either PZT crumbled of the edges of the features or PZT that was present in the polymeric lift off film. The latter can be due to incomplete removal of the excess of the suspension after the casting step.

Table 3  
Composition of features sintered on alumina in air atmosphere for 2 h at different temperatures.

T (°C)	Component	Feature	Ratio Zr/Ti
1000	Pb	0.32	1.6
	Zr	0.42	
	Ti	0.26	
1100	Pb	0.00	1.9
	Zr	0.65	
	Ti	0.35	
1200	Pb	0.00	1.4
	Zr	0.58	
	Ti	0.42	

Samples sintered at three different temperatures. The ratio between Zr/Ti in the untreated powder is 1.1. All sintered samples show an increased ratio in favour of Zr.

The composition measured by EDX is given in Table 3 showing a decreasing amount of lead while sinter temperature increases. When sinter temperatures are above 850 °C, lead evaporation takes place from PZT.<sup>19</sup> At 1100 °C no lead is found on the surface. The evaporation of lead also influences the zirconium/titanium ratio (ratio of the untreated powder is 1.1/1.0). The ratio in the first 500–1000 nm (penetration depth of EDX) changes in favour of zirconium. This is observed in all the samples sintered in air on alumina, although the ratio is not constant and peaking at 1100 °C (ratio zirconium/titanium is 1.9/1.0). At 1100 °C all the lead has disappeared from the surface. It is believed that at 1200 °C some rearrangement of the zirconate and titanate takes place resulting in a less distorted ratio.

A cross-section of a sample sintered at 1000 °C is analyzed and the results are shown in Fig. 5. The relative lead and titanium concentrations decrease throughout the film from the substrate side to the air side of the sample, while the relative zirconium concentration increases towards the air side. This concentration gradient of the sample is caused by lead evaporation from the surface while this lead evaporation influences the relative elemental concentration throughout the sample. The zirconium concentration increases significantly from substrate side (bottom) to air side (top). This concentration profile can be attributed to the higher activity of lead zirconate compared to lead titanate.<sup>20</sup> Therefore, it is assumed that lead evaporation takes place pre-

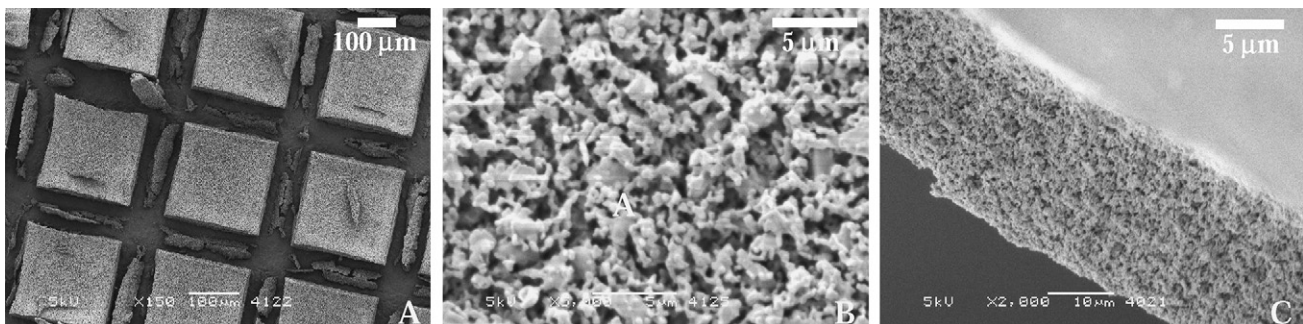


Fig. 4. SEM micrographs of sintered features in air atmosphere for 2 h at 1200 °C. Top view (A), surface (B), cross-section (C).

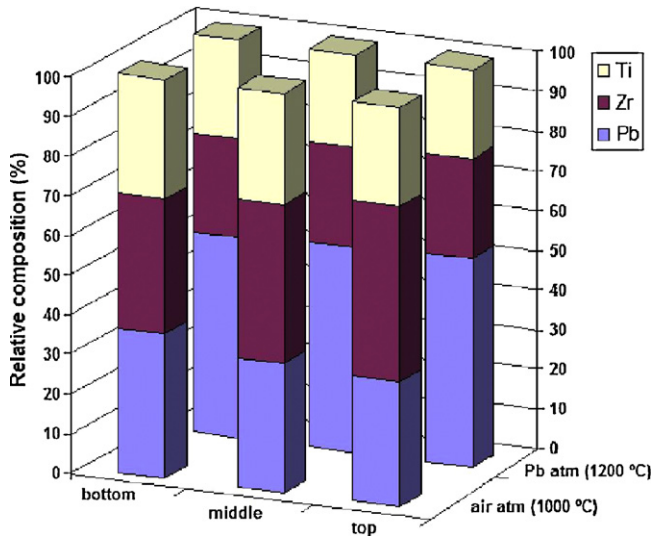


Fig. 5. Relative composition profile of a PZT sample sintered in air atmosphere for 2 h at 1000 °C and 3 h at 1200 °C in lead atmosphere. The  $x$ -axis shows the position in the substrate. The thickness of the sample is 30  $\mu\text{m}$ . The bottom composition is measured close to the substrate and the top composition close to the top surface of the sample. EDX analysis is carried out using a window of 2  $\mu\text{m}$  by 20 mm.

dominantly from the lead zirconate. The lead zirconate phase segregates to the surface and lead evaporates from the surface leaving a lead oxide deficient surface layer.<sup>21</sup> It is assumed that lead evaporation drags lead zirconate from the bulk towards the surface, changing the original ratio between zirconium and titanium in favour of zirconium and increasing the relative amount of titanium in the bulk.

#### 3.4. Sintering on alumina in lead atmosphere

To keep the composition of the sintered features equal to the starting composition of the powder, sintering is carried out in lead atmosphere. At first PZT powder is added to the crucible to supply for the lead environment. However after EDX analysis the samples still show lead loss. Therefore, to prevent lead evaporation, lead zirconate which has a higher vapour pressure than lead zirconate titanate is used. The composition of the samples sintered in lead atmosphere from lead zirconate is given in Table 4. The zirconium/titanium ratio is similar for all the three

Table 4

Composition of features sintered on alumina in lead atmosphere for 2 h at different temperatures.

$T$ (°C)	Component	Feature	Ratio Zr/Ti
1000	Pb	0.53	1.4
	Zr	0.27	
	Ti	0.20	
1100	Pb	0.52	1.4
	Zr	0.28	
	Ti	0.20	
1200	Pb	0.51	1.4
	Zr	0.28	
	Ti	0.21	

sintering temperatures, but is slightly higher than the ratio in the starting powder.

In Fig. 5 it can be seen that the composition of a feature sintered in lead atmosphere hardly changes throughout the sample. The zirconium content is constant and the lead and titanium ratio differs slightly. The small increase in lead content towards the top surface can be caused by condensation from the lead atmosphere. The deviation however is within the experimental error of the measurement.

SEM micrographs of a sample sintered in lead atmosphere are shown in Fig. 6. The features maintain their sharply edged shape. The top surface shows sintered PZT grains comparable to SEM micrographs of the surface of uniaxially pressed-sintered PZT samples.<sup>22,23</sup> The composition of the PZT is almost identical to the composition of the starting powder. The surface is completely dense. This is only observed when the features are sufficiently small (side dimensions < 500  $\mu\text{m}$ ). A cross-section displays a porosity of about 3% (Fig. 6C). Stresses generated by shrinkage during sintering result in crack formation in larger features. Both starting powder and sintered features are analyzed by XRD (Fig. 7), and show the same perovskite phase. The pattern is associated with the rhombohedral and the tetragonal phase (ICDD 01-070-4265, 00-050-0346). The additional peaks appearing in the spectrum of the sintered film are caused by the alumina substrate on which the feature is sintered. The sintered features therefore have the desired PZT structure corresponding to the morphotropic phase boundary.

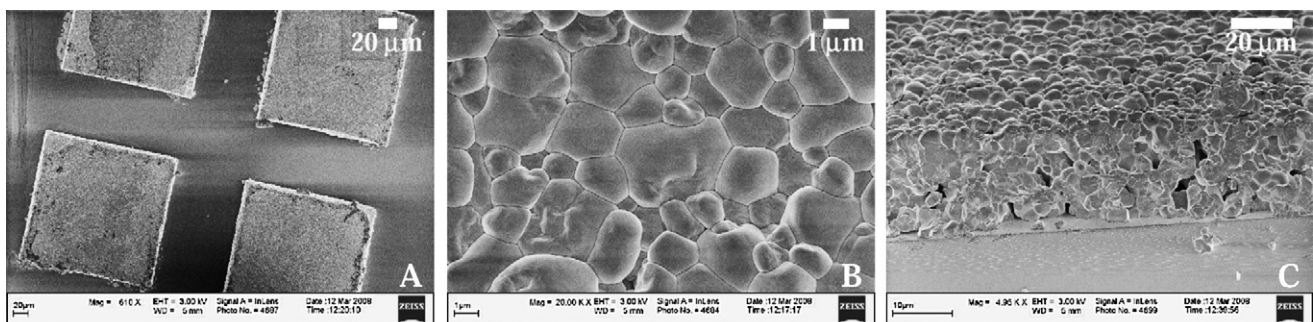


Fig. 6. SEM micrographs of sintered features in lead atmosphere for 3 h at 1200 °C. Top view (A), surface (B), cross-section (C).

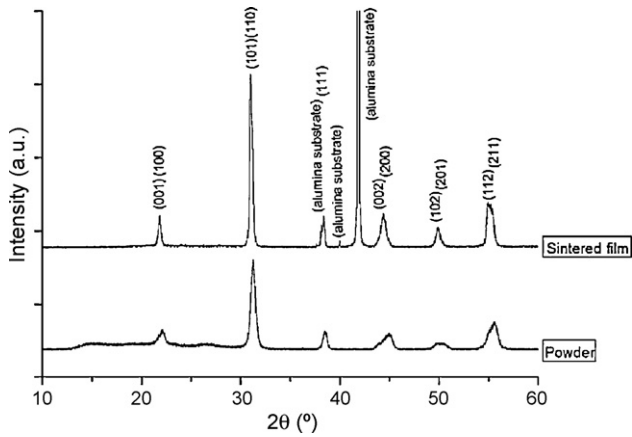


Fig. 7. XRD analysis of unsintered powder and a sintered film. The extra peaks in the sintered film around  $42^\circ$  are caused by the alumina substrate.

### 3.5. Polarization hysteresis loops

Hysteresis properties of PZT were measured using PZT processed in two different ways, respectively samples prepared by isostatic pressing and by tape casting. The relative densities of the isostatically pressed green samples and sintered samples are respectively 71% and 94% of the theoretical density ( $7.87 \text{ kg/dm}^3$ ). The PE-loop, rendered in Fig. 8, shows typical ferroelectric domain switching. The material has a coercive field of  $9.7 \text{ kV/cm}$  and a remanent polarization of  $32.3 \text{ } \mu\text{C/cm}^2$ . From these values the adequacy of the material and sinter procedure is concluded.

To study the hysteresis loops of features made by tape casting, a green tape is sintered on an alumina wafer ( $1200^\circ\text{C}$ , 3 h) in lead atmosphere. The sample is removed from the alumina wafer and electrodes are applied on both sides of the sample, without pretreatment. The coercive field of this film is  $8.8 \text{ kV/cm}$  and the remanent polarization is  $12.3 \text{ } \mu\text{C/cm}^2$ . The polarization of this thin film is significantly lower (2.5 times) than the bulk properties as measured from the sintered discs with thicknesses of  $200\text{--}1400 \text{ } \mu\text{m}$  (Fig. 8).

Surface phenomena are a hypothesis for the difference in performance of the sintered film versus the sintered disc. During sintering lead evaporation from the surface is believed not to be

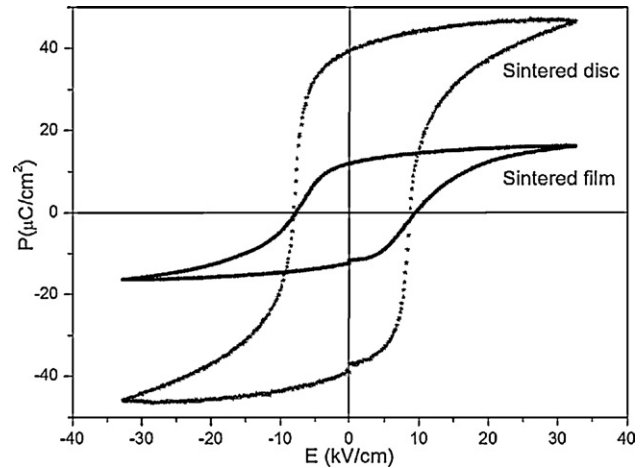


Fig. 8. PE-loops of a sintered disc and a sintered film. Both samples are sintered in lead atmosphere at  $1200^\circ\text{C}$  for 3 h.

completely inhibited. In case of the sintered disc the outer surface exposed to the lead atmosphere is removed by sawing, but this cannot be done for the sintered film. This film has probably a less active surface layer and therefore decreased performance, caused by lead condensation. A second hypothesis is the grain size. Because the preparation method of both PZT samples is different (pressed sample versus tape casting) the grain size differs as well. The average grain size in the sintered disc ( $10 \text{ } \mu\text{m}$ ) is higher than the average grain size in the sintered film from tape casting ( $7 \text{ } \mu\text{m}$ , see Fig. 9). Samples with larger grains show higher remnant and saturated polarization than samples with smaller grains. Next to that samples with smaller grains tend to have a more stretched shape of the hysteresis loop parallel to the  $x$ -axis, which is also clearly visible in the hysteresis loop of the sintered film. In literature, the latter trend was also observed for PZT doped with niobium ( $\text{Pb}_{0.988}(\text{Zr}_{0.52}\text{Ti}_{0.48})\text{Nb}_{0.024}\text{O}_3$ ) although less pronounced.<sup>24</sup> The trend was not observed for undoped PZT, which is the type of PZT used in this research.

Hysteresis loops of PZT features on substrates could not be measured yet because of compatibility problems of the electrodes at high temperatures. This is an area for further investigation.

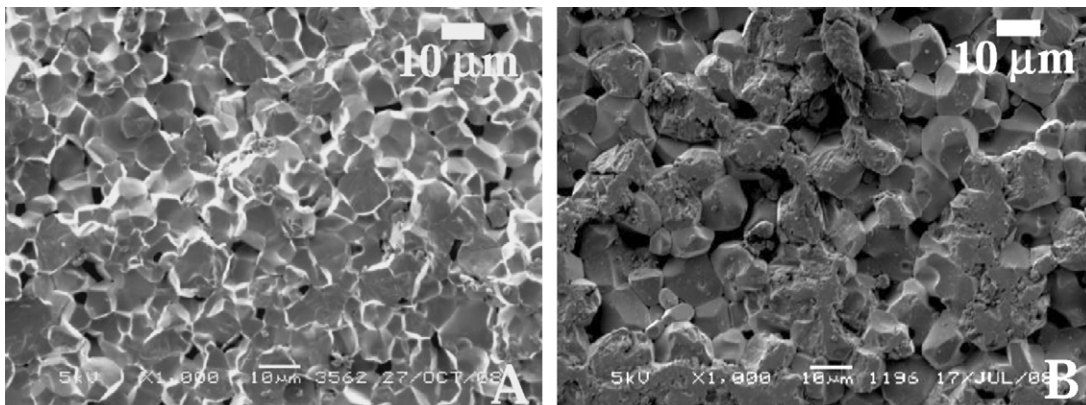


Fig. 9. Cross-section of a sintered film (A) and a sintered disc (B). Both samples are sintered at  $1200^\circ\text{C}$  in lead atmosphere.

#### 4. Conclusion

Freestanding ceramic features are successfully fabricated using a novel simple micromoulding route with good up-scaling opportunities. A PZT suspension is cast on a mould to obtain freestanding structured features. The PZT features are released from the mould by casting a polymeric film over the solidified suspension and releasing the formed composite. It is shown that freestanding squares with lateral dimensions of 200  $\mu\text{m}$  by 200  $\mu\text{m}$  and 40  $\mu\text{m}$  tall are easily fabricated. The support material used during sintering has a strong influence on the final results. Alumina proved to be a good support. Sintering must be performed in lead atmosphere to maintain the initial composition of the PZT. The PZT film prepared via green tape micromoulding has a remanent polarization of 12.3  $\mu\text{C}/\text{cm}^2$  and a coercive field of 8.7 kV/cm. The developed method is unique in its simplicity and can be used to make a wide variety of piezo active structures as well as other ceramics.

#### References

- Bauer, W., Ritzhaupt-Kleissl, H.-J. and Hausselt, J. H., Slip casting of ceramic microcomponents. *Microsyst. Technol.*, 1998, **4**, 125–127.
- Wolny, W. W., Piezoceramic thick films—technology and applications. State of the art in Europe. In *Proceedings of the Twelfth IEEE International Symposium on Application of Ferroelectrics*, 2001, pp. 257–262.
- Rosqvist, T. and Johansson, S., Soft micromoulding and lamination of piezoceramic thick films. *Sens. Actuators, A*, 2002, **97–98**, 512–519.
- Niento, E., Multilayer piezoelectric devices based on PZT. *J. Mater. Sci.*, 1996, **7**, 55–60.
- Schwarzer, S. and Roosen, A., Tape casting of piezo ceramic/polymer composites. *J. Eur. Ceram. Soc.*, 1999, **19**, 1007–1010.
- Navarro, A., Rocks, S. A. and Dorey, R. A., Micromoulding of lead zirconate titanate (PZT) structures for MEMS. *J. Electroceram.*, 2007, **19**, 321–326.
- Heule, M. and Gauckler, L. J., Microfabrication of ceramics based on colloidal suspensions and photoresist masks. *J. Photopolym. Sci. Technol.*, 2001, **14**, 449–452.
- Dorey, R. A., Whatmore, R. W., Beepy, S. P., Torah, R. N. and White, N. M., Screen printed PZT composite thick films. *Intergr. Ferroelectr.*, 2004, **63**, 89–92.
- Brown, R., *RF/Microwave Hybrids*. Kluwer Academic Publishers, Boston, 2003, pp. 93–97.
- Prasad, P. S. R. K., Reddy, A. V., Rajesh, P. K., Ponnamban, P. and Prakasan, K., Studies on rheology of ceramic inks and spread of ink droplets for direct ceramic ink jet printing. *J. Mater. Process. Technol.*, 2006, **176**, 222–229.
- Windle, J. and Derby, B., Ink jet printing of PZT aqueous ceramic suspensions. *J. Mater. Sci. Lett.*, 1999, **18**, 87–90.
- Wang, Z. J., Kokawa, H. and Maeda, R., Electrical properties and microstructure of lead zirconate titanate (PZT) thin films deposited by pulsed-laser deposition. *Ceram. Int.*, 2004, **30**, 1529–1533.
- Miyoshi, T., Preparation of full-dense Pb(ZrTi)O<sub>3</sub> ceramics by aerosol deposition. *J. Am. Ceram. Soc.*, 2008, **91**, 1–7.
- Kamel, T. M. and With, G. d., Poling of hard ferroelectric PZT ceramics. *J. Eur. Ceram. Soc.*, 2008, **28**, 1827–1838.
- Duran, P. and Moure, C., Sintering at near theoretical density and properties of PZT ceramics chemically prepared. *J. Mater. Sci.*, 1985, **20**, 827–833.
- Beepy, S. P., Blackburn, A. and White, N. M., Processing of PZT piezoelectric thick films on silicon for microelectromechanical systems. *J. Micromech. Microeng.*, 1999, **9**, 218–229.
- Belavic, D. and Zarnik, M. S., Properties of lead zirconate titanate thick-film piezoelectric actuators on ceramic substrates. *Int. J. Appl. Ceram. Technol.*, 2006, **3**, 448–454.
- Gebhardt, S., Seffner, L., Schlenkrich, F. and Schönecker, A., PZT thick films for sensor and actuator applications. *J. Eur. Ceram. Soc.*, 2007, **27**, 4177–4180.
- Schönecker, A., Gesemann, H.-J. and Seffner, L., Low-sintering PZT-ceramics for advanced actuators. In *Proceedings of the Tenth IEEE International Symposium on Application of Ferroelectrics*, 1996, pp. 263–266.
- Holman, R. L. and Fulrath, R. M., Intrinsic nonstoichiometry in the lead zirconate–lead titanate system determined by Knudsen effusion. *J. Appl. Phys.*, 1973, **44**, 5227–5236.
- Saha, S. K. and Agrawal, D. C., Composition fluctuations and their influence on the properties of lead zirconate titanate ceramics. *Am. Ceram. Soc. Bull.*, 1992, **71**, 1424–1428.
- Garg, A. and Agrawal, D. C., Effect of net PbO content on mechanical and electromechanical properties of lead zirconate titanate ceramics. *Mater. Sci. Eng. B*, 1998, **56**, 46–50.
- Nersisyan, H. H., Yang, B. S., Kim, B. B., Lee, J. H. and Won, C. W., Combustion synthesis and characterization of spherical powder. *Mater. Lett.*, 2005, **59**, 1066–1070.
- Randall, C. A., Kim, N., Kucera, J.-P., Cao, W. and Shrout, T. R., Intrinsic and extrinsic size effects in fine-grained morphotropic-phase-boundary lead zirconate titanate ceramics. *J. Am. Ceram. Soc.*, 1998, **81**, 677–688.